and some applications. Proc. Natl. Acad. Sci. USA, 76: 4350–4354.

Ulloa, L., Diez-Guerra, F.J., Avila, J. and Diaz-Nido, J. (1994). Localization of differentially phosphorylated isoforms of microtubule-associated protein 1B in cultured rat hippocampal neurons. Neuroscience, 61: 211–223.

Webster, D.R., Wehland, J., Weber, K. and Borisy, G.G. (1990). Detyrosination of alpha tubulin does not stabilize microtubules in vivo. J. Cell Biol., 111: 113–122.

Westermann, S. and Weber, K. (2003). Post-translational modifications regulate microtubule function. Nat. Rev. Mol. Cell Biol., 4: 938–947.

Wohl, C.A. and Weiss, S. (1998). Retinoic acid enhances neuronal proliferation and astroglial differentiation in cultures of CNS stem cell-derived precursors. J. Neurobiol., 37: 281–290.

Wolff, A., Denoulet, P. and Jeantet, C. (1982). High level of tubulin microheterogeneity in the mouse brain. Neurosci. Lett., 31: 323–328.

Yoshida, K., Arai, T., Yokota, T., Komatsu, N., Miura, Y., Yanagisawa, K., Tetsuka, T. and Tominaga, S. (1995). Studies on natural ST2 gene products in the human leukemic cell line UT-7 using monoclonal antihuman ST2 antibodies. Hybridoma, 14: 419–427.

J. Biochem. **136**, 81–87 (2004)
DOI: 10.1093/jb/mvh103

Protective Properties of Neoechinulin A against SIN-1–Induced Neuronal Cell Death

Kiyotoshi Maruyama, Takashi Ohuchi, Kenji Yoshida, Yasushi Shibata, Fumio Sugawara and Takao Arai*

Department of Applied Biological Science, Faculty of Science and Technology, Tokyo University of Science, Yamazaki 2641, Noda 278-8510

Received February 24, 2004; accepted April 30, 2004

Peroxynitrite ($ONOO^-$) is thought to be involved in the neurodegenerative process. To screen for neuroprotective compounds against $ONOO^-$-induced cell death, we developed 96-well based assay procedures for measuring surviving cell numbers under oxidative stress caused by 3-(4-morpholinyl) sydnonimine hydrochloride (SIN-1), a generator of $ONOO^-$, and sodium *N,N*-dietyldithiocarbamate trihydrate (DDC), an inhibitor of Cu/Zn superoxide (O_2^-) dismutase. Using these procedures, we obtained a microbial metabolite that rescued primary neuronal cells from SIN-1-induced damage, but not from DDC-induced damage. By NMR analysis, the compound was identified as neoechinulin A, an antioxidant compound that suppresses lipid oxidation. We found that the compound rescues neuronal cells such as primary neuronal cells and differentiated PC12 cells from damage induced by extracellular $ONOO^-$. However, non-neuronal cells, undifferentiated PC12 cells and cells of the fibroblast cell line 3Y1 were not rescued. Neoechinulin A has scavenging, neurotrophic factor–like and anti-apoptotic activities. This compound specifically scavenges $ONOO^-$, but not O_2^- or nitric oxide (NO). Similar to known neuroprotective substances such as nerve growth factor and extracts of *Gingko biloba* leaves, neoechinulin A inhibits the SIN-1-induced activation of caspase-3–like proteases and increases NADH-dehydrogenase activity. These results suggest that neoechinulin A might be useful for protecting against neuronal cell death in neurodegenerative diseases.

Key words: free radical scavengers, neoechinulin A, neuroprotective effect, oxidative stress, peroxynitrite.

Peroxynitrite ($ONOO^-$) is produced from superoxide (O_2^-) and nitric oxide (NO) (*1*). O_2^- is highly toxic to neurons as it initiates the chain-reactive production of various reactive oxygen species (ROS) during metabolism; protection against O_2^--induced toxicity is critical for neuronal survival (*2*, *3*). NO has diverse physiological functions (*4–7*) and is toxic to neuronal cells (*8*). NO reacts with O_2^- in a diffusion-limited manner to form the more toxic oxidant $ONOO^-$ (*1*), which induces the death of PC12 cells (*9–11*) and cortical neurons (*12*). In the central nervous system, $ONOO^-$ can be generated by microglial cells activated by pro-inflammatory cytokines or β-amyloid peptide and by neurons (*13*). $ONOO^-$ is far more selective than other strong oxidant and preferentially reacts with thiols (*14*). In addition, $ONOO^-$ also reacts with tyrosine to yield 3-nitrotyrosine (*15*). Increasing levels of nitrotyrosine (*16*) are associated with degenerating neurons in the Alzheimer's disease brain, suggesting pathogenic roles for $ONOO^-$.

SIN-1 (3-(4-morpholinyl) sydnonimine hydrochloride) is a vasodilator that spontaneously releases O_2^- and NO into the medium, thereby producing $ONOO^-$ (*17*, *18*). The compound causes a concentration-dependent increase in cortical cell injury (*19*). It has been reported that neurotrophic factors such as nerve growth factor (NGF) (*20*), and free radical scavengers such as uric acid (*21*) and manganese (III) tetrakis (4-carboxyphenyl) porphyrin (Mn-TBAP) (*22*), rescue neuronal cells from SIN-1-induced damage. However, these compounds prevent oxidative damage caused by various ROS as well as $ONOO^-$ -induced damage.

Copper/zinc superoxide dismutase (Cu/Zn-SOD) is highly expressed in neurons (*23*). Thus, an SOD-inhibitor, sodium *N,N*-dietyldithiocarbamate trihydrate (DDC) elevates the amounts of intracellular O_2^- and induces oxidative damage through the chelathor of Cu^{2+} in the active site of Cu/Zn-SOD (*24*, *25*). To obtain compounds that specifically protect neuronal cells against $ONOO^-$-induced oxidative damage, we screened microbial metabolites that rescue primary neuronal cells from SIN-1-induced injury, but not from DDC-induced injury. We obtained a microbial metabolite that specifically protects against $ONOO^-$-induced cell death. In this paper, we describe the neuroprotective properties of this compound.

MATERIALS AND METHODS

Culture of Fungi and Extraction of Their Metabolite— Fungi were isolated as described by Inoue *et al.* (*26*) and incubated at room temperature for 21 d. Each culture was filtered through cheesecloth to remove the mycelia, and the components were extracted with CH_2Cl_2. The

*To whom correspondence should be addressed. Tel: +81-4-7122-9387, Fax: +81-4-7123-9767, E-mail: takarai@rs.noda.tus.ac.jp

organic extract was evaporated *in vacuo* to yield a crude extract, which was subjected repeatedly to silica gel column chromatography using *n*-hexane–ethyl acetate as the solvent.

Cell Culture and 96-Well Based Assay Procedures—Primary neuronal cells were prepared from embryonic 17-d Wister rat brains as described by Suzumura *et al.* (*27*). In brief, the meninges were removed and the brains were dissociated by adding in Dulbecco's modified Eagle's medium (DMEM) MIXTURE F-12 HAM (Sigma Aldrich Fine Chemicals, St. Louis, MO, USA) containing 2.85 mg/ml glucose, 5 μM HEPES, 25 μg/ml insulin, 2 μM progesterone, 0.1 mM putrescine, 0.03 μM sodium selenite, 0.1 mg/ml apo-transferrin, 100 U/ml penicillin and 100 μg/ml streptomycin (DF medium).

For screening microbial metabolites, primary neuronal cells were cultured on poly-D-lysine (PDL) coated 96-well plastic plates (Becton Dickinson, NJ, USA) at an initial density of 0.7×10^5 cells/cm^2 in 2% fetal bovine serum (FBS)–DF medium for 5 d at 37°C. The cultures were treated with microbial metabolites for 24 h, and then, cell death was induced by adding 1 mM SIN-1 (Dojindo, Kumamoto Japan) or 4 μg/ml DDC (Wako, Osaka, Japan). After 24 h, and live cells were counted using a Cell Counting Kit-8 (Dojindo). The kit detects mitochondrial NADH-dehydrogenase activity in live cells by measuring the reduction of the tetrazolium monosodium salt, WST-8. This is a modified MTT assay, and it is known that the MTT assay is not influenced in the presence of various oxidants. Cell number was also measured by the CyQUANT Cell Proliferation Assay Kit (Molecular Probes, Eugene, USA), which quantifies the amount of DNA (*28*). The chemical structures of the compounds obtained were determined by NMR analysis.

PC12 cells were incubated in 75-cm^2 tissue culture flasks in DMEM (Nissui, Tokyo, Japan) supplemented with 10% FBS, 5% horse serum (HS), 100 U/ml penicillin, and 100 μg/ml streptomycin. NGF-differentiated PC12 cells were treated with 100 ng/ml NGF for 5 d. Cells of the rat fibroblast cell line 3Y1 were cultured in DMEM containing 10% FBS, 100 U/ml penicillin, and 100 μg/ml streptomycin.

To study the protective effects of microbial metabolites and known scavengers on PC12 cells and 3Y1 cells, cells were cultured at a initial density of 3.0×10^3 cells/cm^2 in DMEM supplemented with 10% FBS, 5% HS or DMEM containing 10% FBS 5 d at 37°C. Cell death induced by SIN-1 and cell viability were measured as described above.

All cultures were maintained at 37°C in a humidified CO_2-incubator.

Observation of Tyrosine Nitration by Immunofluorescence—Primary neuronal cells were cultured for 7 d on PDL-coated 8-well culture slides (Becton Dickinson). The cells were fixed with 4% paraformaldehyde in PBS (+) (phosphate-buffered saline containing 0.9 mM Ca^{2+} and 0.5 mM Mg^{2+}) for 1 h, washed three times with PBS (+), and incubated with 10% FBS-PBS (+) at 4°C for 1 h. Next, they were incubated with an anti-nitrotyrosine antibody 1AE (Upstate, VA, USA) in 10% FBS-PBS (+) at 4°C for 1 h. After two washes with PBS (+), the cells were incubated with fluorescein isothiocyanate (FITC)-conjugated goat anti-mouse IgG (H&L) (ICN Pharmaceuticals, Inc. Morgan, Irvine, CA, USA) in 10% FBS-PBS (+) for 1 h. Cell nuclei were stained with 10 μg/ml of 4′,6-diamidino-2-phenylindole (DAPI) (Sigma Aldrich Fine Chemicals) at 37°C for 30 min. The cells were then washed with PBS (+), and the nuclear DNA was observed under a fluorescence microscope IX70 (OLYMPUS, Tokyo, Japan).

Measurement of Scavenging Activity—We measured $ONOO^-$ and O_2^- scavenging activities using the chemiluminescent procedure described by Radi *et al.* (*29*) and Beauchamp and Fridovich (*30*), respectively. In brief, 400 mM 5-amino-2,3-dihydro-1,4-phthalazinedione (luminol) (Sigma Aldrich Fine Chemicals) was diluted with 5 mM $NaHCO_3$, pH 10.5 (Wako) in Hank's balanced salt solution (HBSS) (Invitrogen Corp, Carlsbad, CA, USA) (solution A). Test compounds were diluted with HBSS (pH 7.0) (solution B). Solutions A and B and 0.5 mM SIN-1 diluted with HBSS (pH 7) were mixed, and then $ONOO^-$ was measured using a chemiluminometer (MicroLumat LB96V; Berthold Technology, Bad Wildbad, Germany) for 20 min. O_2^- was generated by the xanthine-xanthine oxidase system following the modified method of Beauchamp and Fridovich (*30*). Specimens in Tris-HCl buffer were added to the wells of 96-well plates, each well containing 10 U/ml xanthine oxidase and 2 μM 2-methyl-6-(*p*-methoxyphenyl)-3,7-dihydriimidazo-[1,2-α]pyrazin-3-one (MCLA; Tokyo Kasei Co. Ltd, Tokyo, Japan). To generate O_2^-, 30 μM xanthine was added to each well. Chemiluminescence intensity was measured with a chemiluminometer for 10 min. NO scavenging activity was measured by the fluorometric method of Kojima *et al.* (*31*). The fluorometric detection of NO was carried out using the NO indicator (NONOate; Dojindo) and diaminofluorescein-2 (DAF-2; Daiichi Pure Chemicals Co. Ltd, Tokyo, Japan). The fluorescence from DAF-2T, the reaction product of DAF-2 with NO, was measured as the fluorescence intensity of DAF-2T using a microplate fluorescence reader (Packard Instrument Co., Meriden, USA) (Ex = 490 nm and Em = 520 nm). Mn-TBAP (Dojindo), a scavenger of $ONOO^-$ and O_2^-, and 2-(4-carboxyphenyl)-4,4,5,5-tetramethylimidazoline-1-oxyl 3-oxide (C-PTIO, Dojindo), a scavenger for NO, were used as controls.

Caspase Activity Assay—We measured caspase-3 activity according to Zhou *et al.* (*32*). After exposure to $ONOO^-$, cells were incubated in 50 mM Tris-HCl buffer (pH7.4) containing 4 mM DTT (Sigma Aldrich Fine Chemicals), 2 mM EDTA, 10% glycerol, 0.1% Triton X-100 and 20 μM Ac-Asp-Glu-Val-Asp-7-amido-4-methylcoumarine (Sigma Aldrich Fine Chemicals), a fluorogenic substrate for caspase-3. The activity of caspase-3-like proteases was determined by measuring the fluorescence intensity of the cleaved substrate in a microplate fluorescence reader (Packard Instrument Co., Meriden, USA) (Ex = 360 nm and Em = 460 nm).

RESULTS

Screening of Microbial Metabolites That Prevent SIN-1-Induced Neuronal Cell Death—We screened two hundred microbial metabolites and obtained one compound that rescued primary neuronal cells from SIN-1-induced death. This compound was identified as neoechinulin A by NMR analysis. In the presence of SIN-1, the viability

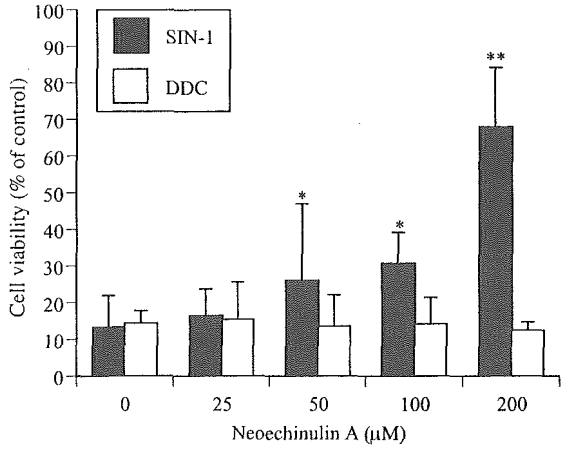

Fig. 1. **Dose-dependent effects of neoechinulin A on neuronal cells.** Primary neuronal cells were seeded at a density of 1.4×10^5 cells/cm^2. After 5 d, cells were incubated with neoechinulin A for 24 h, and treated with 1 mM SIN-1 or 4 μg/ml DDC for 24 h. Cell viability was measured using a Cell Counting Kit-8 (means ± SD, n = 4). $^*p < 0.05$, $^{**}p < 0.01$.

of primary neuronal cells was less than 15%. Treatment with 200 μM neoechinulin A increased cell viability to more than 60%, while such treatment provided no protection against cell death induced by DDC (Fig. 1). This indicates that neoechinulin A protects primary neuronal cells against $ONOO^-$-induced death, but not against O_2^--induced death.

3Y1 cells, a fibroblast cell line, were not rescued from SIN-1–induced death by neoechinulin A. To determine the protective specificity of neoechinulin A, its effect on NGF-differentiated and undifferentiated PC12 cells was examined. Neoechinulin A rescued only differentiated PC12 cells (Fig. 2), suggesting that protective properties of the compound are specific to neuronal cells. Differentiated PC12 cells were also dose-dependently rescued by neoechinulin A (Fig. 3.). The results, shown in the Figures 2 and 3, were confirmed using another cell counting kit, the CYQUANT Cell proliferation kit (data not shown).

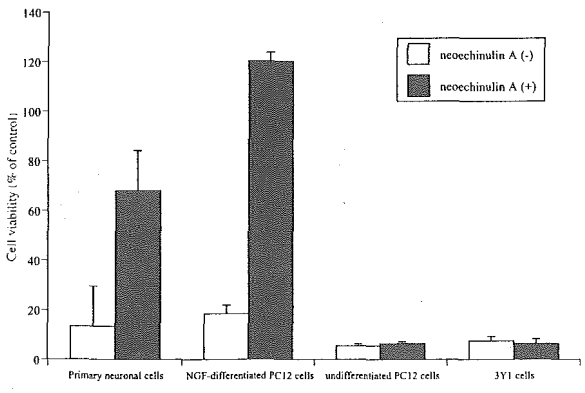

Fig. 2. **Preventive effect of neoechinulin A against SIN-1 injury.** Primary neuronal cells (1.4×10^5 cells/cm^2), PC12 cells (3.0×10^3 cells/cm^2) and 3Y1 cells (3.0×10^3 cells/cm^2) were cultured on PDL-coated 96-well plates for 5 d. After treatment with or without 200 μM neoechinulin A for 24 h, cells were cultured in the presence of 1 mM SIN-1 for 24 h. Cell viability was determined using a Cell Counting Kit-8.

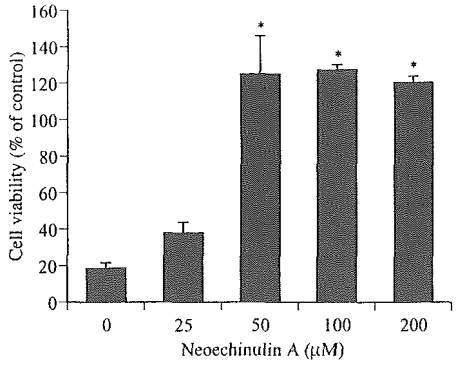

Fig. 3. **Dose-dependent effects of neoechinulin A on differentiated PC12 cells.** PC12 cells were seeded at a density of 3.0×10^3 cells/cm^2 and treated with 100 ng/ml NGF for days. Differentiated PC12 cells were incubated with neoechinulin A for 24 h, and treated with 1 mM SIN-1 for 24 h. Cell viability was measured using a Cell Counting Kit-8. (means ± SD, n = 4) $^*p < 0.01$.

Ability of Neoechinulin A to Scavenge ROS Produced by SIN-1—To study the scavenging activity of neoechinulin A, we examined the nitration of tyrosine residues in SIN-1–exposed cells by immunostaining with monoclonal anti-nitrotyrosine antibody 1AE. Tyrosine nitration was almost completely inhibited by neoechinulin A (Fig. 4), suggesting that neoechinulin A has $ONOO^-$ scavenging activity. This activity was confirmed by the chemiluminescence procedure. The $ONOO^-$ scavenging activity of neoechinulin A is comparable to the activities of Mn-TBAP and C-PTIO (Fig. 5A). Scavenging either O_2^- or NO also prevents the generation of $ONOO^-$ from SIN-1. Mn-TBAP and SOD scavenge about 100% and 75%, respectively of O_2^-, while neoechinulin A does not scavenge O_2^- (Fig. 5B). The fluorometric procedure using DAF-2 revealed that C-PTIO scavenges about 60% of NO, while neoechinulin A does not eliminate NO (Table 1). These results indicate that neoechinulin A specifically scavenges $ONOO^-$, but not O_2^- and NO.

Neuroprotective Effects of Neoechinulin A in SIN-1-Induced Oxidative Stress—It has been reported that various substances, such as anti-apoptotic compounds and neurotrophic factors, have neuroprotective activities (*33*, *34*). We confirmed the neuroprotective effect of the scavengers, C-PTIO and uric acid (Fig. 6A). To examine the activities of neoechinulin A other than scavenging activity, differentiated PC12 cells were pretreated with neoechinulin A, C-PTIO and uric acid for 24 h, and then, after removal of the compounds, with SIN-1 for 24 h. Under these conditions, the scavengers did not rescue differentiated PC12 cells. As shown in Fig. 6B, neoechinulin A still had a neuroprotective effect. This result suggests that neoechinulin A activities other than its scavenging activity.

Figure 3 shows that the viability of neoechinulin A–treated cells was increased by 120%. In this study, live cells were counted with a cell counting kit that measures NADH-dehydrogenase activity as described in "MATERIALS AND METHODS." Several researchers have reported that NGF and bFGF increase the mitochondrial NADH-

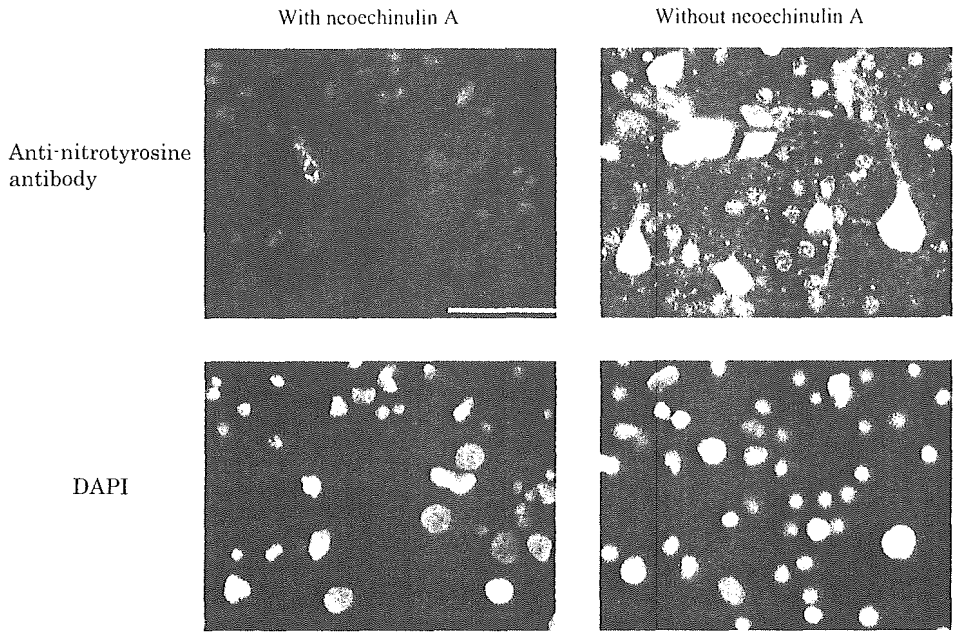

Fig. 4. **Prevention of ONOO⁻-induced tyrosine nitration by neoechinulin A.** Primary neuronal cells were incubated with 0.25 mM SIN-1 for 2 h with or without 200 μM neoechinulin A, and stained with an anti-nitrotyrosine antibody 1AE and DAPI as described in "MATERIALS AND METHODS." Bar = 50 μm

dehydrogenase activity of PC12 cells (*35*, *36*). These facts suggest that neoechinulin A activates this enzyme in PC12 cells. To examine this possibility, we investigated the effect of neoechinulin A on NADH-dehydrogenase in differentiated PC12 cells in the absence of SIN-1. NADH-dehydrogenase activity was normalized to the number of cells as measured with the assay kit that counts cell number based on quantification of genomic DNA. A significant increase in NADH-dehydrogenase activity was observed after the addition of neoechinulin A (Fig. 7).

$ONOO^-$ activates caspase-3 (*37*, *38*). Thus, we examined the effect of neoechinulin A on the SIN-1–induced activation of caspase-3-like proteases in differentiated PC12 cells. The activation was suppressed by about 65% by 200 μM neoechinulin A. On the other hand, neoechinulin A did not influence the caspase-3–ike protease activity of 3Y1 cells (Fig. 8). These results indicate that neoechinulin A has neurotrophic factor-like and anti-apoptotic activities.

DISCUSSION

Neoechinulin A is a known metabolite of *A. rubber* and *A. amstelodami* (*26*). Yagi *et al.* (*39*) reported neoechinulin A to be an antioxidant compound that suppresses lipid peroxidation in dried bonito flakes, *Katsuobushi*. However, additional properties of the compound were not investigated. In this paper, we show that neoechinulin A has scavenging, neurotrophic factor-like and anti-apoptotic activities. The results shown in Fig. 5 and Table 1 indicate that the compond scavenges only $ONOO^-$ released

Table 1. **NO generation in the presence of scavengers.**

Compounds	Generation of NO (% of control)
None	100
Neoechinulin A	100 ± 3
C-PTIO	41 ± 1
SOD	108 ± 5

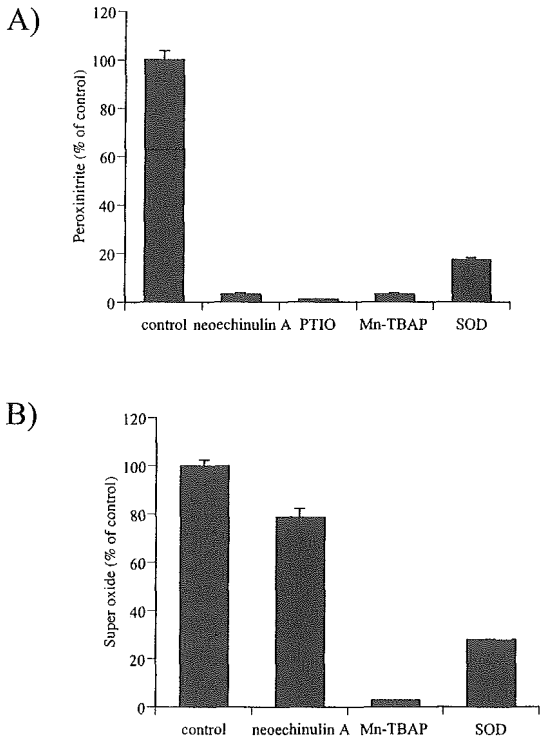

Fig. 5. **Scavenging activity of neoechinulin A.** (A) Measurement of $ONOO^-$ by luminol-dependent chemiluminescence. Luminol was diluted to 400 mM with 5 mM $NaHCO_3$ (pH 10.5) and the samples were diluted with HBSS, pH 7, prior to the measurement of chemiluminescence. Just before measurement, 0.5 mM SIN-1 diluted with HBSS, pH7, was added, and the amount of $ONOO^-$ was measured by a chemiluminometer for 20 min. (B) Measurement of O_2^- by luminol-dependent chemiluminescence. Samples in 100 μl of Tris-HCl buffer, pH 7.4, containing 10 U/ml xanthine oxidase were incubated in a 96-well plate, and 1 μM of MCLA (50 μl) were added. Xanthine (30 μM, 50 μl) was added to generate O_2^-, and the amount of $ONOO^-$ was measured by a chemiluminometer for 20 min.

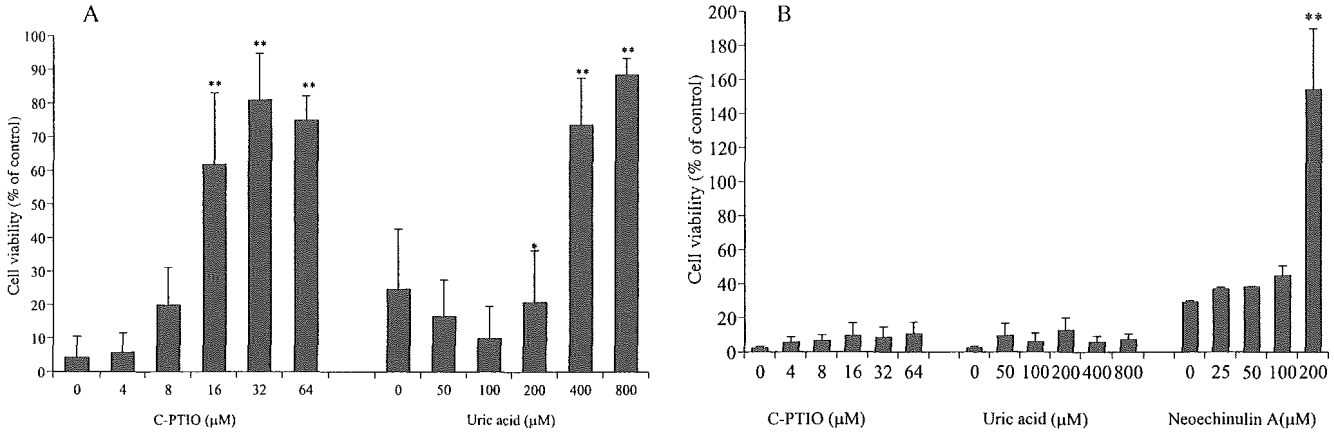

Fig. 6. **Neuroprotective effect of neoechinulin A and scavengers.** PC12 cells were seeded at a density of 3.0×10^3 cells/cm^2 and treated with 100 ng/ml NGF for 5 d. Cell viability was measured using a Cell Counting Kit-8. (A) Cells were incubated with scavengers for 24 h, and treated with 1 mM SIN-1 for 24 h. (B) Cells were incubated with neoechinulin A for 24 h. The neoechinulin A was removed and the cells were treated with 1 mM SIN-1 for 24 h. (means ± SD, $n = 4$) $^*p < 0.05$, $^{**}p < 0.01$.

from SIN-1. In addition, neoechinulin A specifically protects neuronal cells against SIN-1–induced cell death (Fig. 2). Thus, neoechinulin A is very useful for investigations of $ONOO^-$-induced neuronal cell death.

$ONOO^-$ is a powerful oxidant and cytotoxin whose production has been associated with conditions that result in damage to neurons. The appearance of nitrotyrosine immunoreactivity in postmortem brain from individuals with Parkinson's disease and other neurodegenerative conditions (*40–42*) also serves as indirect evidence of $ONOO^-$ production. It is well known that extracts of *Gingko biloba* leaves (EGb 761) rescue neuronal cells against ROS-induced cell death (*43*, 44). EGb 761 includes two major groups of constituents, flavonoids and terpenoids, that are involved in scavenging and antiapototic activities. It has been reported that EGb 761 increases the level of mRNA for the mtDNA-encoded subunit 1 of NADH-dehydrogenase (*45*) and suppresses the activation of caspase-3 caused by various apoptosis inducers (*46*). In the case of neoechinulin A, one compound has scavenging, neurotrophic factor-like and antiapoptotic activities. It should be noted that neoechinulin A scavenges $ONOO^-$, but not NO, because NO has various physiological functions (*4–7*). Therefore, neoechinulin A may be useful for protection against $ONOO^-$-induced neuronal cell death in neurodegenerative diseases.

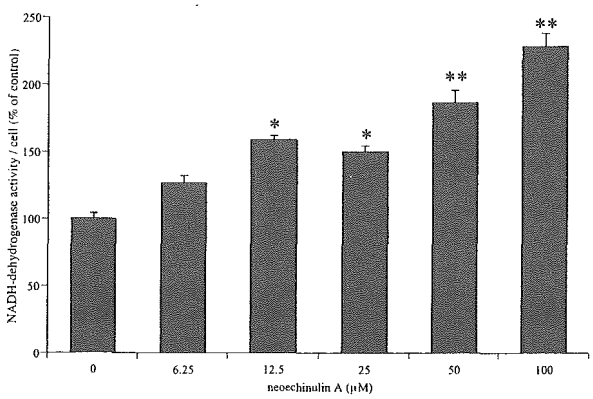

Fig. 7. ***Effect of neoechinulin A on the NADH-dehydrogenase activity of PC12 cells.*** PC12 cells were seeded at a density of 3.0×10^3 cells/cm^2 and treated with 100 ng/ml NGF for 5 d. The indicated concentration of neoechinulin A was added to each well and the relative NADH-dehydrogenase activity per cell was determined as described in "MATERIALS AND METHODS" (means ± SD, $n = 4$). $^*p < 0.05$, $^{**}p < 0.01$.

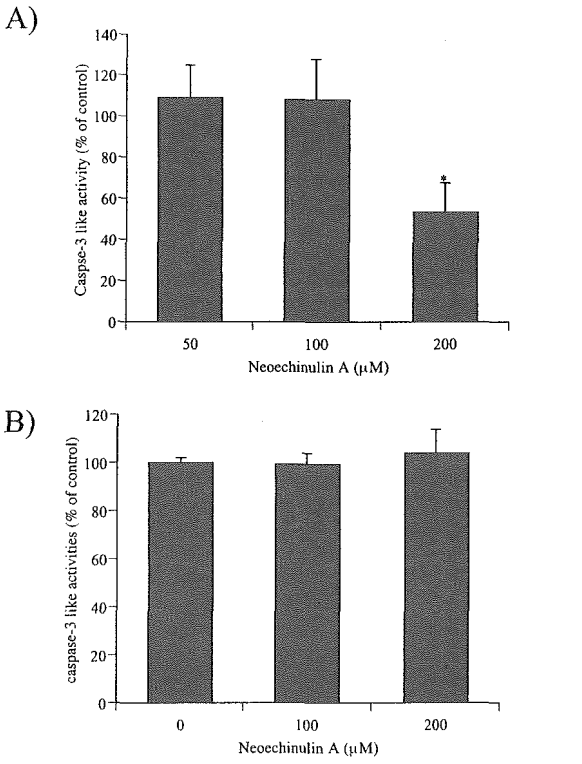

Fig. 8. ***Effect of neoechinulin A on caspase-3 like protease activity.*** PC12 cells (A) and 3Y1 cells (B) were seeded at a density of 3.0×10^3 cells/cm^2. PC12 cells were treated with 100 ng/ml NGF. Five days later, the cells were incubated with neoechinulin A for 24 h. After removal of the neoechinulin A, 0.5 mM SIN-1 was added. After 3 h, caspase activity was measured as described in "MATERIALS AND METHODS" (means ± SD, $n = 4$). $^*p < 0.01$.

This research was supported in part by grants for Research on Advanced Medical Technology from the Ministry of Health, Labor and Welfare of Japan, and from the Promotion and Mutual Aid Corporation for Private Schools of Japan. We thank Mr. T. Shimada and Miss. Y. Ishihara (Science University of Tokyo) for excellent technical assistance.

REFERENCES

1. Beckman, J.S. (1996) The physiological and pathological chemistry of nitric oxide in *Nitric Oxide* (Lancaster, J.R., ed.) pp.1–82, New York Academic, New York
2. Behl, C., Davis, J.B., Lesley. R., and Schubert, D. (1994) Hydrogen peroxide mediates amyloid beta protein toxicity. *Cell* **77**, 817–827
3. Enokido, Y. and Hatanaka, H. (1993) Apoptotic cell death occurs in hippocampal neurons cultured in a high oxygen atmosphere. *Neuroscience* **57**, 965–972
4. Nathan, C.F. (1992) Nitric oxide as a secretory product of mammalian cells. *FASEB J.* **6**, 3051–3064
5. Schmidt, H.H., Walter, U. (1994) NO at work. *Cell* **78**, 919–925
6. Garthwaite, J. and Boulton, C.L. (1995) Nitric oxide signaling in the central nervous system. *Annu. Rev. Physiol.* **57**, 683–706
7. Yun, H-Y., Dawson, V.L., and Dawson, T.M. (1996) Neurobiology of nitric oxide. *Crit. Rev. Neurobiol.* **10**, 291–316
8. Huang, Z., Huang, P.L., Panahian, N., Dalkara, T., Fishman, M.C., and Moskowitz, M.A. (1994) Effects of cerebral ischemia in mice deficient in neuronal nitric oxide synthase. *Science* **265**, 1883–1885
9. Estévez, A.G., Radi, F., Barbeito, L., Shin, J.T, Thompson, J.A., and Beckman, J.S. (1995) Peroxynitrite-induced cytotoxicity in PC12 cells: evidence for an apoptotic mechanism differentially modulated by neurotrophic factors. *J. Neurochem.* **65**, 1543–1550
10. Troy, C.M., Derossi, D., Prochiantz, A., Greene, L.A., and Shelanski, M.L. (1996) Downregulation of Cu/Zn superoxide dismutase leads to cell death via the nitric oxide-peroxynitrite pathway. *J. Neurosci.* **16**, 253–261
11. Spear, N., Estévez, A.G., Barbeito, L., Beckman, J.S., and Johnson, G.V. (1997) Nerve growth factor protects PC12 cells against peroxynitrite-induced apoptosis via a mechanism dependent on phosphatidylinositol-3 kinase. *J. Neurochem.* **69**, 53–59
12. Bonfoco, E., Krainc, D., Ankarcrona, M., Nicotera, P., and Lipton, S.A. (1995) Apoptosis and necrosis: two distinct events induced, respectively, by mild and intense insults with N-methyl-D-aspartate or nitric oxide/superoxide in cortical cell cultures. *Proc. Natl Acad. Sci. USA* **92**, 7162–7166
13. Torreilles, F., Salman-Tabcheh, S., Guerin, M., and Torreilles, J. (1999) Neurodegenerative disorders: the role of peroxynitrite. *Brain Res. Brain Res. Rev.* **30**, 153–163
14. Radi, R., Beckman, J.S., Bush, K.M., and Freeman, B.A. (1991) Peroxynitrite oxidation of sulfhydryls. The cytotoxic potential of superoxide and nitric oxide. *J. Biol. Chem.* **266**, 4244–4250
15. Ischiropoulos, H., Zhu, L., Chen, J., Tsai, M., Martin, J.C., Smith, C.D., and Beckman, J.S. (1992) Peroxynitrite-mediated tyrosine nitration catalyzed by superoxide dismutase. *Arch. Biol. Chem. Biophys.* **298**, 431–437
16. Smith, M.A., Harris, P.L.R., Sayre, L.M., Beckman, J.S., and Perry, G. (1997) Widespread peroxynitrite-mediated damage in Alzheimer's disease. *J. Neurosci.* **17**, 2653–2657
17. Huie, R.E. and Padmaja, S. (1993) The Reaction of NO with Superoxide. *Free Rad. Res. Commun.* **18**, 195–199
18. Noach, E. and Feelisch, E. (1991) Molecular mechanisms of nitrovasodilator bioactivation. *Basic Res. Cardiol.* **86**, 37–50
19. Trackey, J.L., Uliasz, T.F., and Hewett, S.J. (2001) SIN-1-induced cytotoxicity in mixed cortical cell culture: peroxynitirite-dependent and -independent induction of excitotoxic cell death. *J. Neurochem.* **79**, 445–455
20. Kume, T., Nishikawa, H., Tomioka, H., Katsuki, H., Akaike, A., Kaneko, S., Maeda, T., Kihara, T., and Shimohama, S. (2000) p75-mediated neuroprotection by NGF against glutamate cytotoxicity in cortical cultures. *Brain. Res.* **852**, 279–289
21. Regoli, R. and Winston, G.W. (1999) Quantification of total oxidant scavenging capacity of antioxidants for peroxynitrite, peroxyl radicals, and hydroxyl radicals. *Taxicol. Appl. Pharmacol.* **156**, 96–105
22. Quijano, C., Hernandez-Saavedra, D., Castro, L., McCord, J.M., Freeman, B.A., and Radi, R. (2001) Reaction of peroxynitrite with Mn-superixide dismutase. Role of the metal center in decomposition kinetics and nitration. *J. Biol. Chem.* **276**, 11631–11638
23. Pardo, C.A., Xu, Z., Borchelt, D.R., Price, D.L., Sisodia, S.S., and Cleveland, D.W. (1995) Superoxide dismutase is an abundant component in cell bodies, dendrites, and axons of motor neurons and in a subset of other neurons. *Proc. Natl Acad. Sci. USA* **92**, 954–958
24. Du, J., Suzuki, H., Nagase, F., Akhand, A.A., Ma, X.Y., Yokoyama, T., Miyata, T., Nakashima, .I. (2001) Superoxide-mediated early oxidation and activation of ASK1 are important for initiating methylglyoxal-induced apoptosis process. *Free Radic. Biol. Med.*, **31**, 469–478
25. Cocco, D., Calabrese, L., Rigo, A., Argese, E., and Rotilio, G. (1981) Re-examination of the reaction of diethyldithiocarbamate with the copper of superoxide dismutase. *J. Biol. Chem.*, **256**, 8983–8986
26. Inoue, S., Murata, J., Takamatsu, N., Nagano, H., and Kishi, Y. (1977) Synthetic studies on echinulin and related natural products. V. Isolation, sturucture and synthesis of echinulin-neoechinulin type alkaloids isolated from *Aspergillus amstelodami* (author's transl.). *Yakugaku Zasshi* **97**, 576–581
27. Suzumura, A., Sawada, M., and Marunouti, T. (1996) Selective induction of interleukin-6 in mouse microglia by granulocyte-macrophage colony-stimulating factor. *Brain. Res.* **713**, 192–198
28. Chandrasekher, G., Ma, X., Lallier, T.E., Bazan, and H.E.P. (2002) Delay of corneal epithelial wound healing and induction of keratocyte apoptosis by platelet-activating factor invest. *Ophthalmol. Vis. Sci.* **43**, 1422–1428
29. Radi, R., Cosgrove, T.P., Beckman, J.S., and Freeman, B.A. (1993) Peroxynitrite-induced luminol chemiluminescence. *Biochem. J.* **290**, 51–57
30. Beauchamp, C. and Fridovich, I. (1971) Superoxide dismutase: improved assays and an assay applicable to acrylamide gels. *Anal. Biol.* **44**, 276–287
31. Kojima, H., Nakatsubo, N., Kiuchi, K., Kawahara, S., Kirino, Y., Nagoshi, H., Hirata, Y., and Nagano, T. (1998) Detection and imaging of nitric oxide with novel fluorescent indicators: diaminofluoresceins. *Anal. Chem.* **70**, 2446–2453
32. Zhou, L.J. and Zhu, X.Z. (2000) Reactive oxygen species-induced apoptosis in PC12 cells and protective effect of biobalide. *J. Pharmacol. Exp. Ther.* **293**, 982–988
33. Connner, B. and Dragunow, M. (1998) The role of neuronal growth factors in neurodegenerative disorders of the human brain. *Brain Res. Brain Res. Rev.* **27**, 1–39
34. Satoh, T. (2002) Neurotrophin-like low molecular weight compounds. *Nippon Yakurigaku Zasshi* **120**, 327–334
35. Rhodes, C.H., Nezitis, S.G.E., Gonatas, N.K., and Fleiscier, B. (1989) Selective effect of nerve growth factor on some Golgi and lysosomal enzyme activities of rat pheochromocytoma (PC12) cell. *Arch. Biochem. Biophys.* **272**, 175–184
36. Ohuchi, T., Maruoka, S., Sakudo, A., and Arai, T. (2002) Assay-based quantitative analysis of PC12 cell differentiation. *J. Neurosci. Methods* **118**, 1–8
37. Bao, F. and Liu, D. (2003) Peroxynitrite generated in the rat spinal cord induces apoptotic cell death and activates caspase-3. *Neuroscience* **116**, 59–70
38. Ito, S., Wu, G., Kimoto, T., Hisatomi, T., Ishibashi, T., Rao, N. (2004) Peroxynitrite-induced apoptosis in photoreceptor cells. *Curr. Eye Res.* **28**, 17–24
39. Yagi, Y. and Doi, M. (1999) Isolation of an antioxidative substance produced by *Aspergillus repens*. *Biosci. Biotechnol. Biochem.* **63**, 932–933

40. Good, P.F., Werner, P., Hsu, A., Olanow, C.W., and Perl, D.P. (1996) Evidence of neuronal oxidative damage in Alzheimer's disease. *Am. J. Pathol.* **149**, 21–28
41. Good, P.F., Hsu, A., Werner, P., Perl, D.P., and Olanow, C.W. (1998) Protein nitration in Parkinson's disease. *J. Neuropathol. Exp. Neurol.* **57**, 338–342
42. Heales, S.J., Bolanos, J.P., Stewart, V.C., Brookes, P.S., Land, J.M., and Clark, J.B. (1999) Nitric oxide, mitochondria and neurological disease. *Biochim. Biophys. Acta* **1410**, 215–228
43. Marcocci, L., Maguire, J.J., Droy-Lefaix, M.T., and Paker, L. (1994) The nitric oxide-scavenging properties of *Gingko biloba* extract EGb 761. *Biochem. Biophys. Res. Commun.* **201**, 462–475
45. Marcocci, L., Paker, L., Droy-Lefaix, M.T., Sakaki, A., and Gardes-Albert, M. (1994) Antioxidant action of *Gingko biloba* extract EGb 761. *Methods Enzymol.* **234**, 462–475
46. Tendi, E.A., Bosetti, F., Dasgupta, S.F., Stella, A.A., Drieu, K., and Rapoport, S.I., (2002) Gingko biloba extracts EGb 761 and biobalide increase NADH dehydrogenase mRNA level and mitochondrial respiratory control ratio in PC12 cells. *Neurochem. Res.* **27**, 4319–4323
47. Luo, Y., Smith, J.V., Paramasivam, V., Burdick, A., Curry, K.J., Buford, J.P., Khan, I., Netzer, W.J., Xu, H., and Butko, P. (2002) Inhibition of amyloid-beta aggregation and caspase-3 activation by the Gingko biloba extract EGb761. *Proc. Natl. Acad. Sci. USA* **99**, 12197–12202

イメージングで解き明かす生命機能

第15回 モノクローナル抗体を用いたポリグルタミン酸化チューブリンの神経細胞内局在

新井孝夫 Takao Arai（東京理科大学理工学部応用生物科学科）
E-mail：takarai@rs.noda.tus.ac.jp／URL：http://www.rs.noda.tus.ac.jp/~takarai/

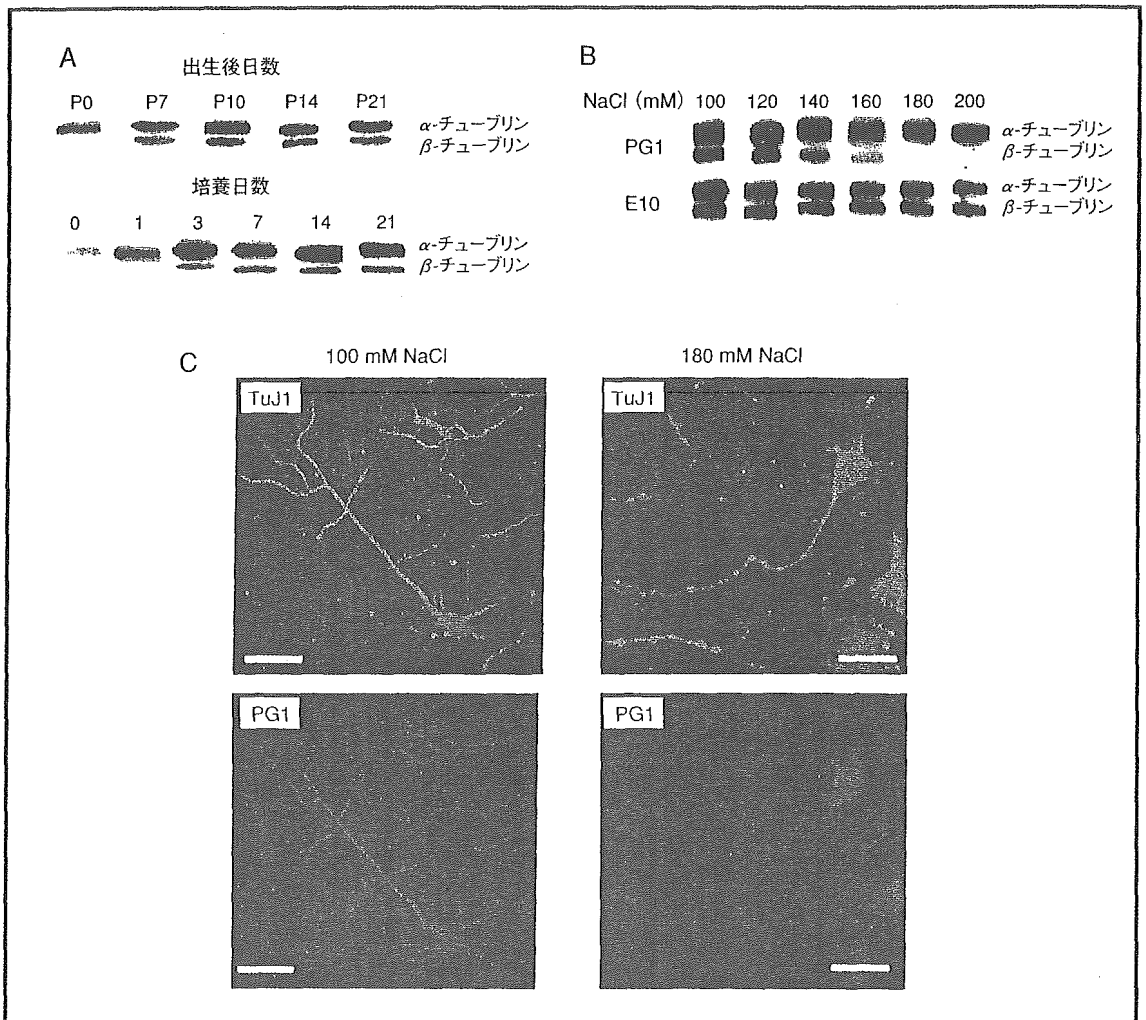

イオン強度による抗体特異性の変化とそれを利用した免疫蛍光染色

A）発達過程を追ったラット脳およびレチノイン酸存在下培養のラット胎仔脳神経幹細胞におけるチューブリンのポリグルタミン酸化を，抗ポリグルタミン酸化チューブリン抗体PG1により解析した．培養1日後には胎仔脳と同様にα-チューブリンが，3日目以降は成熟脳と同様にα-，β-両チューブリンがこの翻訳後修飾を受けた．B）PG1の反応特異性はNaCl濃度に依存し，高塩濃度ではα-チューブリン特異的であった．C）7日培養の神経幹細胞におけるこの修飾チューブリンの局在を，PG1と抗βⅢ-チューブリン抗体TuJ1を用いた二重免疫蛍光抗体法で調べた．100 mMと180 mM NaCl条件下における染色性の相違は，神経突起ではβ-チューブリンのみがポリグルタミン酸化されることを示している．スケールバー：50 μm

背景

α-，β-チューブリンのC末端はグルタミン酸残基の豊富な領域であるが，この領域内のグルタミン酸残基のγ位カルボキシル基に，さらに数個のグルタミン酸残基が付加するポリグルタミン酸化という翻訳後修飾を受ける．モノクローナル抗ポリグルタミン酸化チューブリン抗体の多くは，α-とβ-チューブリンの両者を認識する[1]．多くの臓器や胎仔脳ではα-チューブリンのみがこの修飾を受けているのに対し，成熟脳では両チューブリンが修飾される[2]．現在のところ，この翻訳後修飾を受けたチューブリンの神経細胞内局在の研究は進んでおらず，この翻訳後修飾の果たす役割についての有力な考えも確立されていない．

イメージングが明らかにしたポリグルタミン酸化チューブリンの神経細胞内局在

モノクローナル抗ポリグルタミン酸化チューブリン抗体PG1は，図Aの上に示したように，ラット脳の発達の過程におけるα-，β-チューブリンのポリグルタミン酸化の制御を調べるうえで有用である．また，胎仔脳あるいは成熟脳から神経幹細胞を調製する技術や神経細胞に分化させる培養系は確立されている[3]．そこで，ラット胎仔脳神経幹細胞をレチノイン酸存在下において8ウェルカルチャースライド中で培養し，PG1を用いたウエスタンブロットによりチューブリンのポリグルタミン酸化を調べた．図Aの下に示したように，1日後にはα-チューブリンのみがポリグルタミン酸化され，3日目にはβ-チューブリンの修飾も認められた．β-チューブリンの修飾は，7日目でほぼ一定となった．このことは，この培養系がチューブリンポリグルタミン酸化の研究に有用であることを示している．一方，PG1のα-，β-チューブリンに対する特異性がリン酸緩衝液中のNaCl濃度により変化することを見出した（図B）．すなわち，100 mM NaCl中では両チューブリンを認識したが，180 mM NaCl濃度ではα-チューブリン特異的な反応性を示した．これに対し，同じ抗ポリグルタミン酸化チューブリン抗体E10の場合は，NaCl濃度による反応特異性の変化は起こらなかった．

レチノイン酸存在下で7日培養した神経幹細胞におけるポリグルタミン酸化チューブリンの局在を，この塩濃度変化に依存した抗体特異性の変化を利用して，PG1と神経細胞特異的な抗βⅢ-チューブリン抗体TuJ1を用いた二重免疫蛍光抗体法により観察したのが図Cである．100 mM NaClの染色条件下では細胞体と神経突起の両者が染色されたのに対し，180 mMにおいては細胞体しか染色されなかった．このことは，神経突起においてはβ-チューブリンのみがポリグルタミン酸化されることを示唆している．

翻訳後修飾タンパク質を認識するモノクローナル抗体には，タンパク質特異性の低いものが多い．塩濃度変化によりタンパク質特異性のある反応条件を見出したという本研究結果は，モノクローナル抗体が翻訳後修飾の研究にとって有力な武器となることを改めて示したものと意義づけることができる．

今後の展望と可能性

脳の発達に伴うチューブリンのポリグルタミン酸化の研究から，β-チューブリンのポリグルタミン酸化は神経細胞の成熟と関連すると考えられている．β-チューブリンのポリグルタミン酸化が神経突起において重要な役割を果たしていることを示唆するこの結果は，今後の研究の発展の契機となりうるものである．カチオン性リポソームを用いてモノクローナル抗体を細胞内に導入する技術が開発され，抗チューブリンモノクローナル抗体の導入が細胞増殖を阻害することが示されている[4]．イメージングとこれらの技術を併用することにより，機能解明が大きく進展することが期待される．

〈参考文献〉

1）Wolff, A. et al.：Eur. J. Cell Biol., 59：425-432, 1993
2）Audebert, S. et al.：J. Cell Sci., 107：2313-2322, 1994
3）Takahashi, J. et al.：J. Neurobiol., 38：65-81, 1999
4）Ohuchi, T. et al.：Bioimages, 8：57-64, 2000

Original Article

Neutrophilic involvement in the damage to coronary arteries in acute stage of Kawasaki disease

KEI TAKAHASHI, TOSHIAKI OHARASEKI, SHIRO NAOE, MEGUMI WAKAYAMA AND YUKI YOKOUCHI

Department of Pathology, Ohashi Hospital, Toho University School of Medicine, Tokyo, Japan

Abstract

Background: There has been no morphological evidence that polymorphonuclear leukocytes (PMNL) infiltrate the coronary arterial lesions of acute Kawasaki disease (KD) patients, although clinical data indicate the activation of PMNL.

Methods: The experimental materials consisted of eight autopsy patients who died during the acute phase of KD. Duration of the illness ranged from 6 to 32 days. The tissues were fixed and embedded in paraffin. Hematoxylin and eosin, elastica van Gieson and azan–Mallory stainings were performed for routine histological examination. In addition, antibodies to CD3, CD20, CD68 and neutrophil elastase were used for immunohistochemistry to identify infiltrating cells in arterial lesions.

Results: The inflammatory cells that appeared in the coronary arterial lesions were mainly composed of macrophages in all patients. In addition, numerous neutrophils were also identified in the coronary arterial lesions of the patients who died 10 days after the onset of KD. Neutrophilic infiltration reached a peak earlier than the peaks of CD68+ macrophages, CD3+ T lymphocytes and CD20+ B lymphocytes.

Conclusions: These results suggest that neutrophils are involved in the damage occurring to coronary arteries in the early stage of KD. Vasodilation might occur as a result of injury to vascular walls caused by neutrophils, as well as macrophages.

Key words coronary arteritis, coronary artery aneurysm, immunohistochemistry, Kawasaki disease, neutrophil elastase.

Kawasaki disease (KD) is an acute febrile illness that manifests mainly in infancy and early childhood.[1] The most important complication is coronary arteritis leading to formation of an aneurysm.[2] Although clinical and epidemiological data support an infectious cause of KD, the cause and pathogenesis of this disease remain unclear. Conventional therapy for KD includes high-dose i.v. immunoglobulin (IVIG) and aspirin. The mortality rate, as well as the incidence of coronary artery abnormalities, has decreased since IVIG therapy was started.[3] Therapy with IVIG is obviously effective for KD patients, but this therapy cannot completely prevent the formation of coronary artery aneurysms. The management of KD patients who are non-responsive to IVIG remains controversial.

Recently, an elastase inhibitor has been used in the treatment of KD to inhibit polymorphonuclear leukocyte (PMNL)-elastase activity.[4] Polymorphonucleocytosis in the acute phase of KD suggests involvement of neutrophils in the acute inflammatory process in vascular lesions. PMNL-elastase is significantly elevated in the circulation during the acute phase of KD.[5] The presence of toxic neutrophils is useful as a predictor of coronary risk.[6] Activated PMNL produce a variety of oxidants, proteases and inflammatory cytokines, which may damage endothelial cells, resulting in vascular lesions.[7–9] However, there has been no morphological evidence that PMNL invade the walls of the coronary arteries in the acute phase of KD. Therefore, the present histopathological study was carried out to investigate the presence of PMNL in coronary arterial lesions of autopsy cases in which the patients died during the acute phase of KD.

Correspondence: Kei Takahashi, Department of Pathology, Ohashi Hospital, Toho University School of Medicine, 2-17-6 Ohashi, Meguro, Tokyo 153-8515, Japan. Email: keitak@oha.toho-u.ac.jp

Received 30 March 2004; revised 13 July 2004; accepted 25 October 2004.

Methods

Coronary arteries were obtained from eight autopsy patients who died during the acute phase of KD, ranging from 6 to 32 days after the onset of illness. These patients included five

Table 1 Patients who died of Kawasaki disease

Age	Sex	Time since onset of KD (days)	Cause of death	
5 years 2 months	M	6	Myocarditis	No coronary artery aneurysm
3 months	M	10	Myocarditis	No coronary artery aneurysm
1 year 5 months	M	17	Myocardial infarction	
3 months	F	17	Myocardial infarction	Administered IVIG
8 months	F	23	Cardiac tamponade	Ruptured coronary artery aneurysm
4 months	M	24	Cardiac tamponade	Ruptured coronary artery aneurysm
3 months	F	30	Myocardial infarction	
2 months	M	32	Myocardial infarction	

IVIG, i.v. immunoglobulin; KD, Kawasaki disease.

Table 2 Antibodies and pretreatments used

Antibody to	Clone	Type	Source	Dilution	Pretreatment
CD3	L26	Polyclonal	Dako, Kyoto, Japan	1:100	0.05% pepsin, autoclaving
CD20	KP1	Monoclonal	Dako, Kyoto, Japan	Prediluted	Autoclaving
CD68	NP57	Monoclonal	Dako, Kyoto, Japan	Prediluted	0.05% pepsin
Neutrophil elastase		Monoclonal	Dako, Kyoto, Japan	1:50	

male and three female subjects. Their ages at death ranged from 2 months to 5 years. Only one patient had been given IVIG (Table 1).

Light microscopic examination and immunohistochemistry

First, the tissues were fixed in 10% formalin and embedded in paraffin. Hematoxylin and eosin staining (HE), elastica van Gieson staining (EvG) and azan–Mallory staining were performed for routine histological examination. Next, in order to identify infiltrating cells in arterial lesions, immunohistochemical studies were performed on the paraffin sections using the Simple Stain PO method. The primary antibodies used are listed in Table 2. Endogenous peroxidase activity was blocked with 0.3% H_2O_2 in methanol for 30 min. For some antibodies, antigen availability was enhanced by pretreatment with 0.05% pepsin digestion at 37°C for 30 min or by autoclaving for 5 min in 10 mmol/L citrate buffer at pH 6.0. After overnight incubation with primary antibodies at 4°C, slides were incubated with Simple Stain PO solution (Nichirei, Tokyo, Japan) for 30 min at room temperature. Reactions were visualized with 3,3′-diaminobenzidine as the chromogen with 0.005% H_2O_2, and specimens were counterstained with Mayer's hematoxylin.

Quantitative evaluation of infiltrating cells in the vascular lesions

Each sample was viewed at ×40 high-power fields (HPF), and the number of positive cells for each antibody was counted in 10 randomly selected fields.

Results

Histological findings: case presentations

Case 1 (6th day)

In addition to endothelial cell swelling or detachment, scant inflammatory cells consisting of CD3+ lymphocytes and CD68+ macrophages/monocytes were observed in the slightly thickened intima. Splitting of the internal elastic lamina was rarely seen, and there was no edema or inflammatory cell infiltration in the media. In contrast, a small number of CD68+ positive cells infiltrated the adventitia.

Case 2 (10th day)

Neither aneurysms nor dilations had developed in the coronary arteries. Disruption of the internal elastic lamina, edematous dissociation of the media and inflammatory cells were observed in all layers of the arterial walls. Although CD68+ monocytes/macrophages were distributed in all layers, CD3+ or CD20+ lymphocytes were mainly found in the thickened intima. Moreover, antineutrophil elastase antibody-positive cells were predominantly seen in the media, showing edematous dissociation (Fig. 1).

Cases 3, 4 (both 17th day)

Coronary artery aneurysms had developed in both patients. The normal structures of the coronary arteries, such as the media, internal and external elastic lamina, were completely

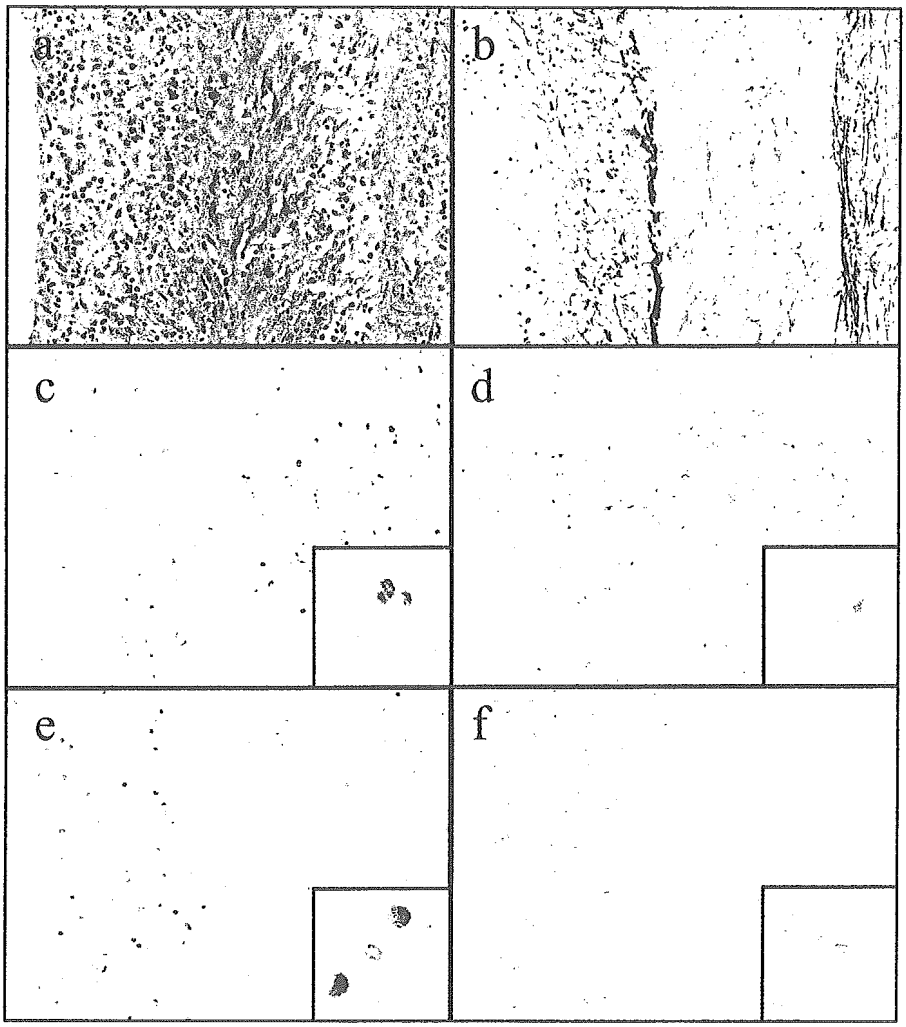

Fig. 1 Coronary artery of the patient who died 10 days after the onset of Kawasaki disease (KD). (a) HE and (b) EvG stains: panarteritis developed, but there was no dilation of the coronary artery. (c) Anti-neutrophil elastase antibody-positive polymorphonuclear leukocytes (PMNL) were predominantly infiltrating the media showing edematous dissociation. (d) CD68-positive monocytes/macrophages were distributed in all layers. (e) CD3 and (f) CD20: both CD3-positive and CD20-positive lymphocytes were mainly infiltrating the thickened intima.

destroyed by severe inflammatory cell infiltration. The predominant cells were CD3+, CD20+ or CD68+ mononuclear leukocytes. Anti-neutrophil elastase antibody-positive PMNL were decreased in number in comparison with that in case 2.

Cases 5, 6 (23rd day and 24th day)

Both patients had died of cardiac tamponade caused by rupture of a coronary artery aneurysm. Proliferation of fibroblasts and smooth muscle cells accompanied by CD68+ macrophages/monocytes and CD3+ lymphocytes was observed in the destroyed aneurysmal wall. However, the lesions contained only a small number of cells positive for anti-neutrophil elastase antibody and CD20 (Fig. 2).

Cases 7, 8 (30th day and 32nd day)

The degree of inflammatory cell infiltration was much milder than in the former cases. Thickened intima, thinned media and adventitia were diffusely replaced by fibrous connective tissue. There was moderate infiltration by CD68+ large mononuclear cells accompanied by a small number of CD3+ lymphocytes in the thickened intima.

Quantification of infiltrating cells in vascular lesions

CD68+ monocytes/macrophages were the most common cells infiltrating the arterial lesions in all patients. The degree of the infiltration was, however, most remarkable in the arterial lesions of patients who died 17 days after the onset. In regard to CD3+ lymphocyte, the cell infiltration in the lesions was the most severe in a patient who died 17 days after the onset of KD. Significant degree of CD20+ lymphocyte infiltration was also seen in the lesions of the same patient who died 17 days after the onset. However, in another patient who died on the 17th illness day and patients who died after that, the level of CD20+ lymphocyte infiltration in the arterial lesions was very low. The number of anti-neutrophil elastase antibody-positive PMNL was the highest in the lesions of the patient who died 10 days after onset. Thereafter, these positive cells gradually became small in number (Fig. 3).

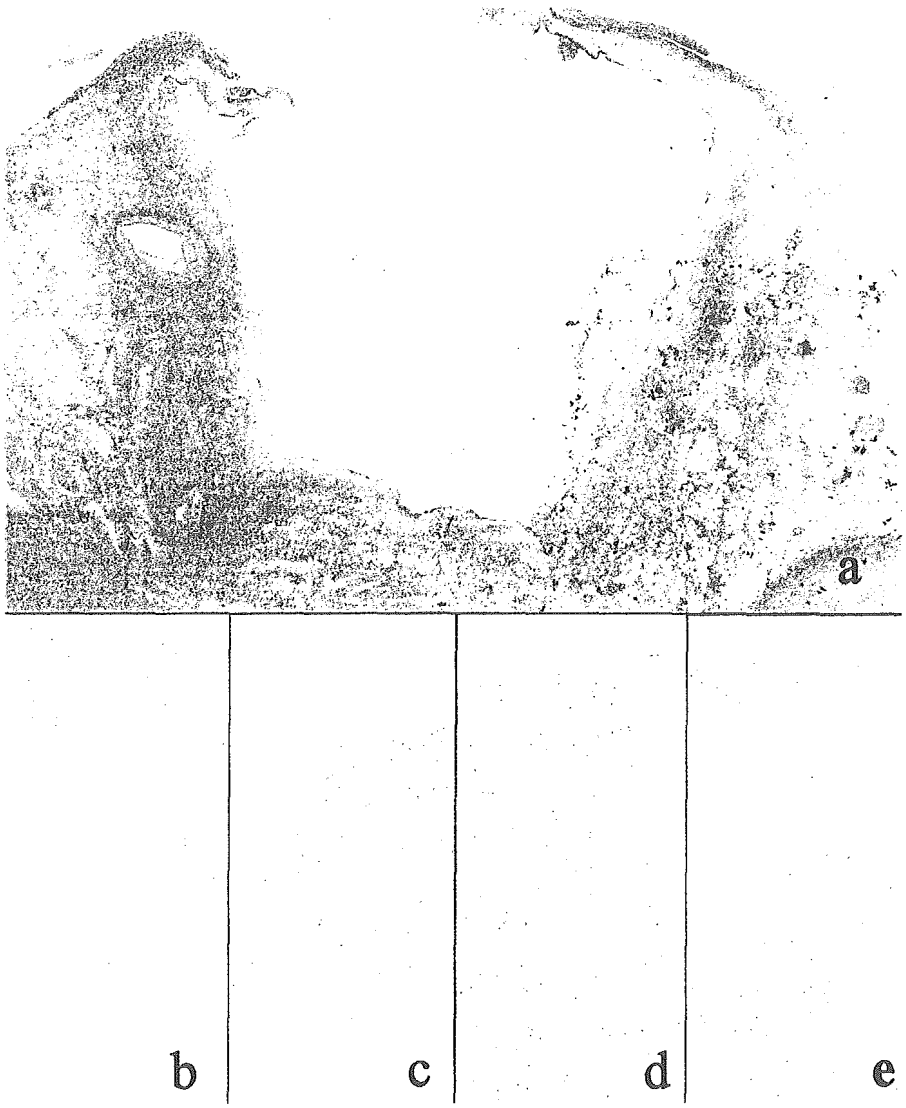

Fig. 2 (a) HE stain: ruptured coronary artery aneurysm of the patient who died 23 days after the onset of Kawasaki disease (KD). Normal arterial structure was completely destroyed by inflammatory cells, and mild fibroblastic proliferation was observed in the adventitia. (b) Only a few antineutrophil elastase antibody-positive cells infiltrated the aneurysmal wall. (c) CD68-positive cells in the lesion were the main component of the infiltrate. (d) CD3 and (e) CD20: moderate and small numbers of positive cells were distributed in the vascular lesions, respectively.

Discussion

We found that the inflammatory cells that appeared in the coronary arterial lesions of each of the KD patients were mainly monocytes/macrophages. Neutrophil infiltration was marked in the patients who died early after the onset of KD, especially in the patient who died on the 10th day of the disease. Neutrophil infiltration reached a peak earlier than the infiltrations of CD68+ monocytes/macrophages, CD3+ lymphocytes and CD20+ lymphocytes. Several investigators reported that neutrophils, lymphocytes and plasma cells as well as macrophages appeared in vascular lesions in the acute phase of KD.[10-13] Unfortunately, there have been no histological reports providing details of the serial changes of these inflammatory cells in the vascular lesions of acute KD. As to the reasons why special attention has not been directed to these cells, KD arteritis is histologically characterized by proliferative granulomatous inflammation accompanied by large mononuclear cells without fibrinoid necrosis. This feature is apparently different from many other types of necrotizing vasculitis, such as classical polyarteritis nodosa, in which significant neutrophilic infiltration with fibrinoid necrosis is important for pathological diagnosis. With regard to another reason, autopsy tissue samples fixed in formalin and embedded in paraffin were inadequate for immunohistochemical examination because of loss of antigenicity. Recently, antibodies that are applicable to those specimens have become commercially available. Therefore, we tried to identify these inflammatory cells using this technique on autopsied materials. Immunohistochemistry for elastase-producing cells was performed to verify neutrophils more accurately and easily. Neutrophils were confirmed by positive granules in the cytoplasm for anti-neutrophil elastase antibody and by the presence of a segmented nucleus stained with hematoxylin.

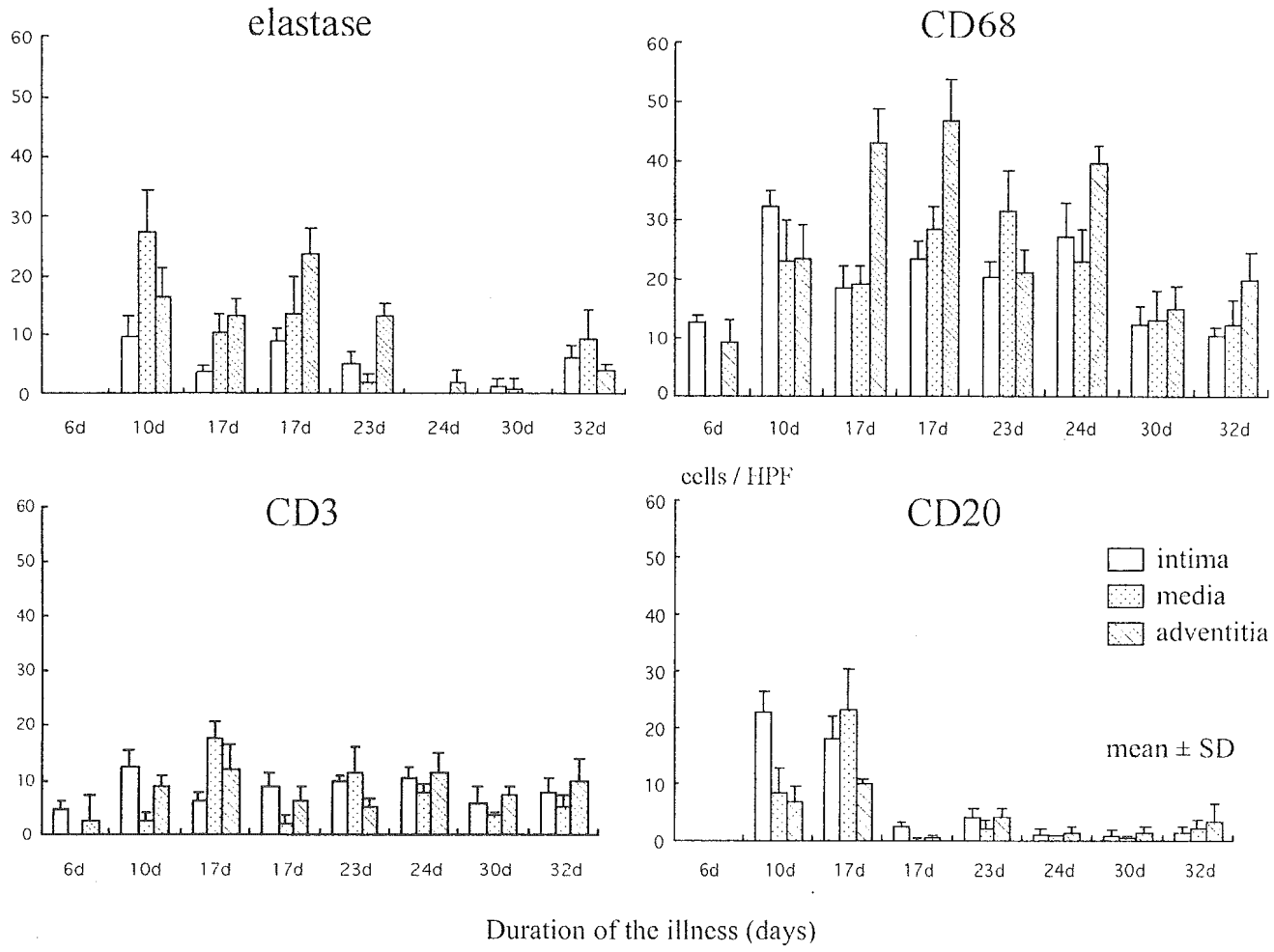

Fig. 3 Change in the numbers of each positive cell according to the duration of Kawasaki disease (KD).

We previously reported that the initial arterial change in KD was edematous dissociation of the media, seen in patients who died as early as 7 days after the onset of KD, and that panarteritis was noted by the 9th day. Dissociation and disruption of the internal elastic lamina could be seen along with panarteritis by the 10th day, and typical inflammatory aneurysms resulting from the mural damage were present within the following 2 days.[10,14] These observations suggest that therapy to reduce arterial inflammation and to prevent the development of coronary artery aneurysms should be administered within the first 10 days after the onset of KD.

In the present study, numerous antineutrophil elastase-positive PMNL appeared in the lesions showing edematous dissociation of the media of the non-aneurysmal coronary arteries of the patient who died 10 days after the onset of KD. This finding suggests that neutrophils are strongly involved in the damaged coronary artery at an early stage of KD. It has been reported that serum levels of inflammatory cytokines such as interleukin (IL)-1, IL-6, tumor necrosis factor (TNF)-α and granulocyte colony-stimulating factor (G-CSF) increase in patients in the acute phase of KD.[7,9] Neutrophils activated by these factors induce the endothelial cell or vascular smooth muscle cell damage. As a result of injury to the vascular walls, vessel dilation might occur. According to this, the arterial lesion seen in this patient seems to correspond to one in a pre-aneurysm stage. It is well known that neutrophils as well as monocytes/macrophages play important roles in the initial host defense mechanisms, but they simultaneously cause tissue damage that is mediated by enzymes secreted by the neutrophils. Proteases may be the primary agents of neutrophil-mediated injury to the vascular walls. Takeshita *et al.* reported that lipopolysaccharide-bound neutrophils released significant amounts of protease into the circulation in all children with KD during the acute phase of the disease.[5]

The mechanism by which high-dose immunoglobulin ameliorates the vasculitis of KD remains obscure. The possibilities include blockade of immunological activation of the

inflammatory response directed to vascular surfaces, saturation of Fc receptors on endothelial cells or phagocytes, or provision of a specific antibody to counteract an unidentified causal agent of KD.[15,16] In contrast, Zaitsu *et al.* reported that ulinastatin, a neutrophil-elastase inhibitor, suppressed new induction of prostaglandin H2 synthase (PHS) mRNA in PMNL. Consequently, immunoglobulin did not suppress new induction of PHS-2 or inhibit TXB2 synthesis.[17] Thus, the mechanism by which inflammation of arterial walls is reduced may be different between immunoglobulin and neutrophil-elastase inhibitors. Okada *et al.* reported that combination therapy using ulinastatin and immunoglobulin was effective in preventing coronary artery complications in KD.[18] Our results indicate that the use of an elastase inhibitor may become an additional or alternative therapeutic approach for KD patients from the histological viewpoint.

Acknowledgments

This work was supported, in part, by The MCLS Study Group, the Japan Kawasaki Disease Research Committee, the Ministry of Health and Welfare, Japan; Grants-in-Aid for Scientific Research from the Ministry of Education, Science and Culture, Japan (14570168, 16590298); and a Grant for Research on Specific Diseases from the Ministry of Health, Labor and Welfare.

References

1 Kawasaki T. Acute febrile mucocutaneous syndrome with lymphoid involvement with specific desquamation of fingers and toes in children. Clinical observation of 50 patients. *Jpn. J. Allergy* 1967; **16**: 178–222.
2 Kawasaki T, Kosaki F, Okawa S, Shigematsu I, Yanagawa H. A new infantile acute febrile mucocutaneous lymph-node syndrome (MLNS) prevailing in Japan. *Pediatrics* 1974; **54**: 271–6.
3 Yanagawa H, Nakamura Y, Yashiro M *et al.* Incidence survey of Kawasaki disease in 1997 and 1998 in Japan. *Pediatrics* 2001; **107**: E33.
4 Nakano M, Yamada S, Hayashi Y, Morishita M, Iwaki T, Toyoda M. Preventive effects of ulinastatin for coronary artery aneurysm formation in Kawasaki disease. In: Kato H (ed.). *Kawasaki Disease*. Elsevier Science, Amsterdam, 1995; 364–71.
5 Takeshita S, Nakatani K, Kawase H *et al.* The role of bacterial lipopolysaccharide-bound neutrophils in the pathogenesis of Kawasaki disease. *J. Infect. Dis.* 1999; **179**: 508–12.
6 Takeshita S, Sekine I, Fujisawa T, Yoshioka S. Studies of peripheral blood toxic neutrophils as a predictor of coronary risk in Kawasaki disease: the pathogenic role of hematopoietic colony-stimulating factors (GM-SF, G-GSF). *Acta Paediatr. Jpn.* 1990; **32**: 508–14.
7 Suzuki H, Noda E, Miyawaki M, Takeuchi T, Uemura S, Koike M. Serum levels of neutrophil activation cytokines in Kawasaki disease. *Pediatr. Int.* 2001; **43**: 115–19.
8 Smedly LA, Tonnesen MG, Sandhaus RA *et al.* Neutrophil-mediated injury to endothelial cells. Enhancement by endotoxin and essential role of neutrophil elastase. *J. Clin. Invest.* 1986; **77**: 1233–43.
9 Inoue Y, Kato M, Kobayashi T, Shinohara M, Sone K, Morikawa A. Increased circulating granulocyte colony-stimulating factor in acute Kawasaki diease. *Pediatr. Int.* 1999; **41**: 330–3.
10 Naoe S, Takahashi K, Masuda H, Tanaka N. Kawasaki disease with particular emphasis on arterial lesions. *Acta Pathol. Jpn.* 1991; **41**: 785–97.
11 Landing HL, Larson E. Pathological features of Kawasaki disease (mucocutaneous lymph node syndrome). *Am. J. Cardiovasc. Pathol.* 1987; **1**: 215–29.
12 Terai M, Kohno Y, Niwa K, Toba T, Sakurai N, Nakajima H. Imbalance among T-cell subsets in patients with coronary arterial aneurysms in Kawasaki disease. *Am. J. Cardiol.* 1987; **60**: 555–9.
13 Rowley AH, Shulman ST, Mask CA *et al.* IgA plasma cell infiltration of proximal respiratory tract, pancreas, kidney and coronary artery in acute Kawasaki disease. *J. Infect. Dis.* 2000; **182**: 1183–91.
14 Masuda H, Naoe S, Tanaka N. A pathological study of coronary artery in Kawasaki disease (MCLS): with special reference to morphogenesis of aneurysm. *J. Jpn. Coll. Angiol.* 1981; **21**: 899–912.
15 Newburger JW, Takahashi M, Burns JC *et al.* The treatment of Kawasaki syndrome with intravenous gamma globulin. *N. Engl. J. Med.* 1986; **315**: 341–7.
16 Nakatani K, Takeshita S, Tsujimoto H, Kawamura Y, Kawase H, Sekine I. Regulation of the expression of Fc-gamma receptor on circulating neutrophils and monocytes in Kawasaki disease. *Clin. Exp. Immunol.* 1999; **117**: 418–22.
17 Zaitsu M, Hamasaki Y, Tashiro K *et al.* Ulinastatin, an elastase inhibitor, inhibits the increased mRNA expression of prostaglandin H2 synthase-type2 in Kawasaki disease. *J. Infect. Dis.* 2000; **181**: 1101–9.
18 Okada M, Nakai S, Kobayashi Y, Satoh T. Effects of intravenous gamma globulin and ulinastatin on patients with Kawasaki disease and predicted giant coronary artery aneurysms. *J. Jpn. Pediatr. Soc.* 1997; **101**: 1165–70.

Cytoplasmic Inclusion Bodies Are Detected by Synthetic Antibody in Ciliated Bronchial Epithelium during Acute Kawasaki Disease

Anne H. Rowley,[1,2] Susan C. Baker,[4] Stanford T. Shulman,[1] Linda M. Fox,[5] Kei Takahashi,[7] Francesca L. Garcia,[1] Susan E. Crawford,[3] Pauline Chou,[3] and Jan M. Orenstein[6]

Departments of [1]Pediatrics, [2]Microbiology/Immunology, and [3]Pathology, Feinberg School of Medicine, Children's Memorial Hospital, Northwestern University, Chicago, and Departments of [4]Microbiology/Immunology and [5]Pathology, Stritch School of Medicine, Loyola University, Maywood, Illinois; [6]Department of Pathology, George Washington University School of Medicine, Washington, DC; [7]Department of Pathology, Toho University School of Medicine, Tokyo, Japan

Background. In developed nations, Kawasaki disease (KD) is the most common cause of acquired heart disease in children. An infectious etiology is likely but has not yet been identified. We have previously reported that oligoclonal immunoglobulin A plasma cells infiltrate acute KD tissues and that synthetic KD antibodies detect a distinctive spheroidal antigen in acute KD ciliated bronchial epithelium.

Methods. To further characterize the antigen in acute KD bronchi, we examined paraffin-embedded ciliated bronchial epithelium using light microscopy (LM) and transmission electron microscopy (TEM).

Results. The spheroids observed by immunohistochemistry (IHC) are visualized as inclusion bodies with hematoxylin-eosin and nucleic acid stains and in methylene blue/azure II/basic fuchsin trichrome–stained plastic sections, suggesting the presence of both protein and nucleic acid. The structures visualized by LM correspond to homogeneous electron-dense perinuclear inclusion bodies (up to 1.4 microns in diameter) in ciliated bronchial epithelium from 4 patients with acute KD examined by TEM. Inclusion bodies were not present in control bronchial epithelium or in nonciliated cells.

Conclusions. The antigen detected in acute KD ciliated bronchial epithelium by IHC with synthetic KD antibodies resides in cytoplasmic inclusion bodies that are consistent with aggregates of viral proteins and associated nucleic acid and may derive from the etiologic agent of KD.

Kawasaki disease (KD) is an acute systemic inflammatory illness of early childhood that particularly affects medium-sized arteries, such as the coronary arteries, and that can result in myocardial infarction, coronary artery aneurysms that rupture, and sudden death [1]. In developed nations, KD has replaced acute rheumatic fever as the most common cause of acquired heart disease in children [2]. Although the etiology is unknown, clinical and epidemiologic data support infection with a ubiquitous microbial agent. This theory predicts that most individuals are asymptomatically infected with the agent during childhood and that only a very small subset of genetically predisposed individuals develop clinical features of KD. In this model, the rarity of KD in infants <3 months old is explained by protective, passive maternal antibodies. The rarity of KD in adults is consistent with widespread immunity. Attempts to identify the etiologic agent of KD by traditional methods have not been successful.

Our laboratory has taken an immunologic approach to the investigation of the etiology of KD. We have discovered that IgA plasma cells infiltrate coronary arteries [3] and other inflamed tissues during acute KD [4] and that, compared with control subjects, peribronchial IgA

Received 20 May 2005; accepted 1 July 2005; electronically published 17 October 2005.

Presented in part: 42nd annual meeting of the Infectious Diseases Society of America, Boston, 30 September–3 October 2004 (abstract 105); 8th International Kawasaki Disease Symposium, San Diego, 17–20 February 2005 (abstract 7); 43rd annual meeting of the Infectious Diseases Society of America, San Francisco, 6–9 October 2005 (abstract 56).

Potential conflicts of interest: none reported.

Financial support: National Institutes of Health (grants K02 HL67011 and R01 HL63771 to A.H.R.); Kawasaki Disease Research Fund of Children's Memorial Hospital.

Reprints or correspondence: Dr. Anne H. Rowley, Professor of Pediatrics and of Microbiology/Immunology, Pediatrics W140, Ward 12-204, 303 E. Chicago Ave., Chicago, IL 60611 (a-rowley@northwestern.edu).

The Journal of Infectious Diseases 2005; 192:1757–66

0022-1899/2005/19210-0013$15.00

plasma cells are significantly increased in the upper respiratory tracts of patients with acute KD, which is similar to findings in children with fatal viral respiratory infections [4]. We have also reported that macrophages and CD8 T lymphocytes are prominent in the inflammatory infiltrate [5]. These immunologic findings suggest the presence of an intracellular pathogen with a respiratory portal of entry.

IgA genes in arteries from patients with acute fatal KD are oligoclonal, that is, are antigen driven [6]. We previously made oligoclonal KD antibodies in vitro and performed immunohistochemical experiments on formalin-fixed, paraffin-embedded tissues from patients with acute KD and from control subjects, and we reported that synthetic KD antibody A identified antigen in acute KD, but not in control, bronchial epithelium as well as in a subset of macrophages in inflamed acute KD tissues, such as the coronary arteries [7]. Antigen was localized to distinctive perinuclear, primarily apical intracytoplasmic "spheroidal bodies" in acute KD ciliated bronchial epithelium by use of synthetic KD antibody A. To further characterize this antigen in acute KD bronchi, we here examine ciliated bronchial epithelium from patients with acute KD by light microscopy (LM) and transmission electron microscopy (TEM).

PATIENTS, MATERIALS, AND METHODS

Patients and specimens. Formalin-fixed, paraffin-embedded lung tissues from patients with fatal acute KD were studied by TEM, because fresh tissue from KD fatalities has been virtually unavailable. Autopsy revealed that patients 1–5 and 7 had coronary artery aneurysms and that patients 8 and 9 had coronary arteritis without aneurysms. Patient 6 had leukemia and developed classic clinical symptoms of acute KD. He developed fatal candidal sepsis 10 days after the onset of KD; autopsy did not reveal evidence of coronary arteritis (table 1). Patients 1, 5, and 7 were included in our previous immunohistochemical study using synthetic KD antibody A [7], as is noted in table 1. Control tissues included formalin-fixed, paraffin-embedded lung tissue from a 3-month-old infant with respiratory syncytial virus (RSV) infection and from a 12-month-old infant with rotavirus infection. We also studied glutaraldehyde-fixed lung tissue from a 1-month-old infant with congenital heart disease and bronchopneumonia and compared the results with those for formalin-fixed, paraffin-embedded lung tissue from the same patient. The present study was approved by the Institutional Review Board of Children's Memorial Hospital.

Synthetic KD antibodies. Synthetic KD antibodies were made as described elsewhere [7]. Immunohistochemistry (IHC) was performed with synthetic antibodies A and J. Antibody J, made from heavy chain 11-5 [6] and light chain 9-8 [7], was prepared after our initial synthetic antibody study and demonstrates strong binding to acute KD ciliated bronchial epithelium. Control synthetic antibody I, made from heavy chain 4-2 [6] and light chain 9-8 [7], does not demonstrate binding to acute KD or control ciliated bronchial epithelium.

IHC. Formalin-fixed, paraffin-embedded tissue sections were deparaffinized by use of xylene, rehydrated, and heated in 10 mmol/L sodium citrate buffer (pH 6.0), to enhance antigen retrieval, as described elsewhere [7]. Sections were incubated with 10–50 μg/mL biotinylated synthetic antibody A, J, or I, and color was developed by use of the Vectastain Elite ABC Kit (Vector). Diaminobenzidine tetrahydrochloride was used as a reaction product, to generate a brown stain. Sections were lightly counterstained with hematoxylin. We recorded positive results when strong brown staining of intracytoplasmic bodies was observed in ciliated bronchial epithelial cells.

Hematoxylin-eosin (HE), Feulgen, methyl green pyronin (MGP), and Fontana stains. Standard HE, Feulgen, MGP, and Fontana staining was also performed on formalin-fixed, paraffin-embedded lung tissue.

TEM. TEM was performed in 2 different laboratories. At Loyola University, resin blocks were made from tissue sections from patients 1, 3, and 4 after IHC with synthetic antibody, to

Table 1. Patients with Kawasaki disease (KD) included in the present study.

Patient (sex, age)	Included in previous study[a] [7]	Ethnicity	Duration of illness before death	Treatment	Cause of death	Year of death
1 (M, 4 months)	Yes (KD7)	White	3 weeks	IVGG, aspirin	Myocarditis	2000
2 (M, 7 months)	No	White	4 weeks	Aspirin	Myocardial infarction	1982
3 (M, 9 months)	No	Unknown	8 weeks	Prednisone	Myocardial infarction	1978
4 (M, 9 months)	No	Japanese	18 days	IVGG, aspirin	Myocardial infarction	1991
5 (M, 6 months)	Yes (KD1)	White	5 weeks	IVHC	Myocardial infarction	1974
6 (M, 6 years)	No	Japanese	10 days	None	Leukemia, candidal sepsis	1981
7 (F, 10 months)	Yes (KD13)	Black	5 weeks	Aspirin	Myocardial infarction	1984
8 (M, 5 years)	No	Japanese	6 days	Aspirin	Myocarditis	1970
9 (F, 19 months)	No	Japanese	29 days	Aspirin	Interstitial pneumonia	1979

NOTE. IVGG, intravenous gammaglobulin; IVHC, intravenous hydrocortisone.

[a] Shown in parentheses are the patient identification nos. from the previous study.

allow for accurate localization of bronchi containing the spheroidal bodies within the lung section. Tissue sections were treated with osmium tetroxide, dehydrated in graded ethanol, and transitioned through propylene oxide into increasing concentrations of epoxy resin. A prepolymerized blank epoxy block was positioned over the area of interest, and the slide was placed into a 60°C oven overnight. The block was snapped off the glass slide after brief contact with dry ice or quick immersion in liquid nitrogen, or both. The block was aligned and thin-sectioned immediately at 80 nm by use of a diamond knife. Sections were picked up on fine bar grids and stained with uranyl acetate and lead citrate, and the grids were viewed on a Hitachi H600 transmission electron microscope at 75 kV.

At George Washington University, pieces of formalin-fixed, paraffin-embedded lung tissue (patient 2) were excised directly from areas of a tissue block containing bronchi that were positive by IHC. The paraffin-embedded tissue was placed on filter paper and warmed to 60°C for 5 min, to remove excess paraffin. To remove the remaining paraffin, the tissue was processed through xylene and decreasing ethanol concentrations and was brought to aqueous PBS neutral buffer. The tissue was then postfixed in osmium tetroxide, processed through graded ethanol and propylene oxide, and embedded in Spurr's epoxy. Semithin (1 micron) plastic sections were cut by use of a glass knife and were stained with the methylene blue/azure II/basic fuchsin trichrome stain for plastic-section LM. The blocks selected for TEM were thinned by use of a diamond knife, stained with uranyl acetate and lead citrate, and examined on a LEO EM10 transmission electron microscope operating at 60 kV.

RESULTS

We noted remarkable similarity between the LM appearance of the KD structures observed by IHC with synthetic KD antibody and intracytoplasmic inclusion bodies of various RNA viruses, such as members of the *Paramyxoviridae* family [8]. We used LM stains and TEM to determine whether intracytoplasmic inclusion bodies were present in acute KD bronchial epithelium and to determine whether, in addition to protein, nucleic acid was a component of the bodies (table 2).

IHC. Dark brown–staining (mostly supranuclear) intracytoplasmic bodies were observed in ciliated epithelial cells of medium-sized bronchi from patients 1–6, 8, and 9 (figures 1 and 2) with synthetic antibodies A and J; these were not observed with control synthetic antibody I. Large bronchi (completely encased by cartilage) and small, nonciliated bronchi generally did not stain with synthetic antibodies A or J. All tissues that were positive with synthetic antibody A were also positive with synthetic antibody J and had the same pattern of staining, although antibody J generally resulted in stronger staining than did antibody A. Ciliated bronchial epithelium from patient 7 did not stain with synthetic antibody A or J, nor did bronchial epithelium from the control subjects. Nonciliated goblet cells (in the same acute KD bronchi in which positive ciliated cells were present) were also negative, as were control bronchi. Although most IHC-positive bronchi showed no evidence of cellular cytotoxicity [7], some bronchi (from patients 4 and 8) did demonstrate acute bronchitis and even necrotizing bronchitis (figure 2). For patient 4, the preserved epithelial cells in damaged bronchi contained antigen (figure 2).

HE. Relatively subtle, round to oval intracytoplasmic perinuclear inclusion bodies could be observed in medium-sized bronchi from patients 1, 2, 4–6, 8, and 9 when stained with HE and examined by LM (figure 1). The inclusion bodies often were amphophilic (staining with both eosin and hematoxylin), suggesting that they contained both protein and nucleic acid. No inclusion bodies were observed for patients 3 and 7 or in control bronchial epithelium.

Fontana stains for lipofuscin. Close analysis of HE-stained sections of bronchial epithelium from several patients with acute KD (patients 4–6) revealed the presence of irregular, golden yellow, granular supranuclear pigment resembling classic lipofuscin in ciliated bronchial epithelial cells (figure 1). Furthermore, in addition to the typical spheroidal bodies, IHC revealed pleomorphic, supranuclear, dark brown–staining material with synthetic antibodies A and J (figures 1 and 2) but not with control synthetic antibody I, suggesting that the antibody was also staining lipofuscin bodies. Therefore, we also performed Fontana staining for lipofuscin. For patients 3, 5, and 6, typical black, supranuclear, granular, lipofuscin staining of the ciliated epithelial cells was observed. However, the level of Fontana staining was much less than the amount of golden yellow granular pigment observed by HE staining and the pleomorphic material stained by IHC. This indicated that the Fontana stain was staining only a relatively small portion of what appeared to be classic lipofuscin in HE sections and suggested that the material that resembled lipofuscin but that was not detected by Fontana stain was KD antigen revealed by IHC. Fontana staining was negative for patients 4 and 7 and in control bronchial epithelium.

Feulgen and MGP stains. On the basis of staining of other cells that can serve as an internal control, the color balance of both the Feulgen and MGP stains appeared to be suboptimal. Nevertheless, the stains clearly delineated the inclusion bodies, indicating that they likely contained nucleic acid. However, because of the suboptimal staining, it was not possible to determine whether the nucleic acid was RNA or DNA. This could have resulted from prolonged initial formalin fixation and/or fixation under acid conditions.

Semithin plastic sections. Perinuclear inclusion bodies were observed in semithin plastic sections from the only patient (patient 2) for whom tissue was retrieved from a paraffin block for TEM. They appeared dark blue with the methylene blue/azure

Table 2. Results of experiments with acute Kawasaki disease (KD) ciliated bronchial epithelial cells.

Patient	IHC with synthetic KD antibody	Stain				TEM
		HE	Fontana[a]	Feulgen	MGP	
1	Positive	ICI	ND	ND	ND	ICI (IHC and TEM show bodies in same location in cell)
2	Positive	ICI, shedding of bronchial epithelium	ND	ND	ICI	Rare ICI (STPS also shows ICI [dark blue])
3	Positive (veins, alveolar septal cells, and interstitial macrophages also positive)	Normal appearance	Positive	Negative	Negative	ICI (ICI also present in interstitial cells)
4	Positive	ICI, LF, necrotizing bronchitis	Negative	ICI	ICI	Rich in electron-dense bodies of various sizes, including ICI
5	Positive	LF, shedding of bronchial epithelial cells	Positive	Rare ICI	Negative	ND
6	Positive	ICI, LF	Positive	ICI	ICI	ND
7	Negative	Bronchitis	Negative	Negative	ND	ND
8	Positive	ICI, bronchitis	ND	ND	ND	ND
9	Positive	ICI	ND	ND	ND	ND

NOTE. HE, hematoxylin-eosin; ICI, intracytoplasmic inclusion bodies; IHC, immunohistochemistry; LF, lipofuscin (golden yellow granular pigment); MGP, methyl green pyronin; ND, not done; STPS, semithin plastic sections (methylene blue/azure II/basic fuchsin trichrome stain); TEM, transmission electron microscopy.

[a] Fontana is a stain for lipofuscin.